

# Circumstellar Nebulae in Young Supernova Remnants

You-Hua Chu\*

\*Astronomy Department, University of Illinois, 1002 W. Green Street, Urbana, IL 61801

**Abstract.** Supernovae descendent from massive stars explode in media that have been modified by their progenitors' mass loss and UV radiation. The supernova ejecta will first interact with the *circumstellar* material shed by the progenitors at late evolutionary stages, and then interact with the *interstellar* material. Circumstellar nebulae in supernova remnants can be diagnosed by their small expansion velocities and high  $[\text{N II}]/\text{H}\alpha$  ratios. The presence of circumstellar nebulae appears ubiquitous among known young supernova remnants. These nebulae can be compared to those around evolved massive stars to assess the nature of their supernova progenitors. Three types of archeological artifacts of supernova progenitors have been observed in supernovae and/or young supernova remnants: (1) deathbed ejecta, (2) circumstellar nebulae, and (3) interstellar bubbles. Examples of these three types are given.

## INTRODUCTION

Massive stars end their lives in supernova explosions, but it is not known exactly at which evolutionary stages massive stars explode. SN 1987A was the only supernova that had a known progenitor, Sk-69°202 [1], and its B3I spectral type was as shockingly different from theorists' expectation as could be. It was eventually recognized that Sk-69°202 was probably a binary, and the companion played a vital role in the stellar mass loss and stellar evolution before the supernova explosion [2]. At present, our knowledge of the transition from massive star to supernova is sketchy as best.

Massive stars lose mass throughout their lives in the forms of fast and slow winds. The mass loss rate heightens particularly toward the late evolutionary stages. The ejected stellar material has been detected as "circumstellar nebulae" around Wolf-Rayet (WR) stars, luminous blue variables (LBVs), and blue supergiants (BSGs) [3,21]. The circumstellar nebulae around these stars are visible because these stars have stellar winds to compress the circumstellar material into dense shells and UV fluxes to ionize the nebulae. It is observed that circumstellar nebulae around different types of stars have different sizes, expansion velocities, and abundances, depending on the history of the stellar mass loss [5].

Circumstellar nebulae can also be detected in young SNRs before they are completely shredded beyond recognition by SNR shocks. The best known example of circumstellar material in a young SNR is the quasi-stationary flocculi (QSFs) in Cas A [6]. Noting a similarity in the kinematic properties and  $[\text{N II}]/\text{H}\alpha$  line ratios between these QSFs and the Galactic WR nebula NGC 6888, Kirshner and Chevalier [6] suggested that the progenitor of Cas A was a WN star. Similarly, if circumstellar nebulae are detected in other young SNRs, the physical properties of these nebulae can be compared to those of known nebulae around massive stars in order to determine the nature of the supernova progenitors.

In this paper, I will first give a brief review on the mass loss from massive stars and how the mass loss modifies the gaseous environment, then describe the different types of circumstellar nebulae and interstellar bubbles that young SNRs interact with, and finally give examples of young supernovae or SNRs that show such “archeological artifacts” of their massive progenitors.

## EVOLUTION, MASS LOSS, AND BUBBLES OF MASSIVE STARS

The most massive stars, with  $M_{\text{ZAMS}} > 40 M_{\odot}$ , will evolve along the sequence  $\text{O} \rightarrow \text{Of} \rightarrow \text{H-rich WN} \rightarrow \text{LBV} \rightarrow \text{H-poor WN} \rightarrow \text{H-free WN} \rightarrow \text{WC} \rightarrow \text{supernova}$  [7]. The less massive stars, on the other hand, evolve through the red supergiant (RSG) phase instead of the LBV phase [8]. Of these different evolutionary stages, fast stellar winds ( $> 1,000 \text{ km s}^{-1}$ ) are seen in main sequence O stars, WR stars, and BSGs; moderately fast winds ( $< 1,000 \text{ km s}^{-1}$ ) are seen in LBVs; and slow winds ( $\sim 20 \text{ km s}^{-1}$ ) are seen in RSGs.

These various stellar winds interact with the ambient medium and form wind-blown bubbles [9]. The hydrodynamic evolution of these bubbles has been calculated for stars evolving along the sequence  $\text{O star} \rightarrow \text{LBV} \rightarrow \text{WR star}$ , e.g., a  $60 M_{\odot}$  star [10], and for stars evolving along the sequence  $\text{O star} \rightarrow \text{RSG} \rightarrow \text{WR star}$ , e.g., a  $35 M_{\odot}$  star [11].

The results of these calculations can be summarized as follows. Massive stars form “interstellar bubbles” during the main sequence stage, as the bubbles consist of mainly interstellar material. The copious mass loss during the LBV or RSG phase forms a small, slowly-expanding, circumstellar nebula within the cavity of the interstellar bubble. During the final WR phase, the fast stellar wind sweeps up and compresses the circumstellar material to form a “circumstellar bubble,” which consists of mainly ejected stellar material.

Interstellar and circumstellar bubbles have both been observed around WR stars, LBVs, and BSGs [5]. Interstellar and circumstellar bubbles can be easily distinguished according to their patterns of expansion and abundances – circumstellar bubbles show regular expansion patterns and high N/O abundance ratios. In general, interstellar bubbles are large, up to a few tens of pc in radius. Circumstellar bubbles of WR stars are usually a few pc in radius and expand fast,  $V_{\text{exp}} \geq 50$

km s<sup>-1</sup>. Circumstellar bubbles of LBVs are small,  $\leq 1$  pc in radius; some expand slowly,  $V_{\text{exp}} < 30$  km s<sup>-1</sup>, while others expand fast with  $V_{\text{exp}} \sim 50\text{--}100$  km s<sup>-1</sup>.  $\eta$  Car is the most extreme but rare case [12].

## DIAGNOSTICS OF CIRCUMSTELLAR NEBULAE

Circumstellar nebulae consist of material ejected by stars. Therefore, the nebular expansion is usually regular and shows point-symmetry with respect to the central star. Furthermore, the elemental abundances show enrichment in CNO products, i.e., high N/O ratios [13]. For normal nebular conditions, a high N abundance leads to high [N II]/H $\alpha$  line ratios. It is thus easy to diagnose a circumstellar nebula using the expansion pattern and [N II]/H $\alpha$  ratios.

Circumstellar nebulae in young SNRs can be detected using high dispersion spectroscopic observations of the H $\alpha$  and [N II]  $\lambda 6548$  lines. The presence of a narrow emission component with anomalously high [N II]/H $\alpha$  ratio would indicate the existence of a circumstellar nebula.

## CIRCUMSTELLAR NEBULAE AND INTERSTELLAR BUBBLES IN YOUNG SNRS

Young SNRs contain a rich variety of archeological artifacts left behind by their massive progenitors. Three distinct types of circumstellar and interstellar nebulae have been observed: (1) deathbed ejecta, (2) circumstellar nebulae, and (3) interstellar bubbles. Descriptions and examples of these nebulae are given in the subsections below.

### 1. Deathbed Ejecta

Some supernovae, after the supernova light has faded, show narrow emission lines from circumstellar nebulae that are characterized by very high densities,  $\gg 10^6$  H-atom cm<sup>-3</sup>, and moderate expansion velocities,  $< 100$  km s<sup>-1</sup>. The best examples are SN 1987K [14], SN 1997ab [15], and SN 1997eg [16]. The H $\alpha$  and [N II] lines of SN 1978K and SN 1997ab are shown in Figure 1.

The H $\alpha$ + [N II] spectrum of SN 1978K shows a narrow, nebular H $\alpha$  component superposed on the peak of the broad H $\alpha$  component of the SN ejecta. The narrow nebular [N II]  $\lambda\lambda 6548, 6583$  lines are also detected. The velocity profiles of the nebular components imply an expansion velocity  $< 50$  km s<sup>-1</sup>. The [N II]/H $\alpha$  ratio is  $\sim 1$ . This nebular emission must originate from a circumstellar nebula. Low-dispersion spectra suggest a nebular density of a few  $\times 10^5$  H-atom cm<sup>-3</sup> [17].

The H $\alpha$  spectra of SN 1997ab and SN 1997eg both have a narrow, nebular, P Cygni profile superposed on the broad profile of the SN ejecta [15,16]. The

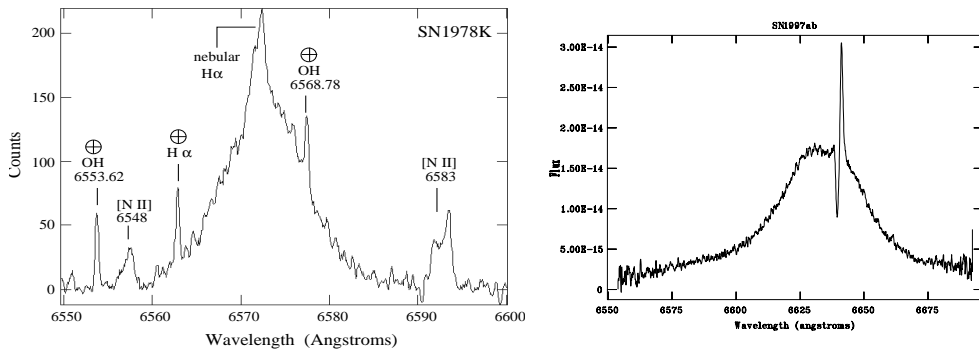


**FIGURE 1. Left:** High-dispersion  $H\alpha$ + $[N II]$  spectrum SN 1987K, taken from [14]. **Right:** High-dispersion  $H\alpha$  spectrum of SN 1997ab, taken from [15].

$[N II]/H\alpha$  ratio of the nebular component is high (Salamanca, private communication), and the expansion velocity of the nebular component is  $< 100 \text{ km s}^{-1}$  [15,16], suggesting the existence of a circumstellar nebula. The P Cygni profile of the nebular component requires that the density is  $\geq 10^7 \text{ H-atom cm}^{-3}$ .

The densities of the circumstellar nebulae around these three supernovae are orders of magnitude higher than the densities observed in circumstellar bubbles of WR stars [14]. The density of SN 1978K’s circumstellar nebula is comparable to those of the densest LBV nebulae, but the densities of SN 1997ab’s and SN 1997eg’s circumstellar nebulae are higher than any known circumstellar nebulae. These circumstellar nebulae, therefore, must have a different origin from the known circumstellar nebulae around evolved massive stars. They may represent the stellar material ejected shortly prior to the supernova explosion, justifying the name “deathbed ejecta.”

It would be of great interest to determine the elemental abundances of these circumstellar nebulae, and compare them to the nucleosynthesis yields of stellar evolution models. The results will shed light on the evolutionary stage of the SN progenitor.

## 2. Circumstellar Nebulae

### *The Case of SN 1987A*

The first example given here is SN 1987A, where we are witnessing the collision between supernova ejecta and a circumstellar nebula. HST WFPC2 images of SN 1987A taken after the SN light had faded away revealed an inner ring and two outer rings (Figure 2). The  $[N II]/H\alpha$  ratios of these rings are 4.2 and 2.5 for the inner and outer rings, respectively [18]. These high  $[N II]/H\alpha$  ratios suggest anomalous nitrogen abundance, indicating that these rings are circumstellar, as opposed to interstellar, in origin. The expansion velocity of the inner ring is  $\sim$

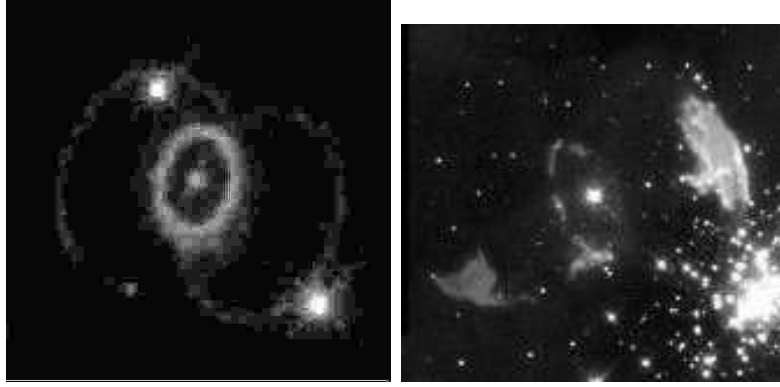


**FIGURE 2. Left:** SN 1987A and its circumstellar rings. **Right:** Sher 25 and its circumstellar rings. The progenitor of SN 1987A, Sk–69 202, was a B3 I star and Sher 25 is a B1.5 I star. Both inner rings are 0.4 pc in diameter!

$10 \text{ km s}^{-1}$ , indicating that it was not ejected during the SN explosion [19]. The morphology and kinematics of these circumstellar rings place constraints on the SN progenitor’s mass loss history and lend support to its binarity [2].

It is interesting to note that circumstellar rings around B supergiants similar to those of SN 1987A’s are probably rare. Only one case has been serendipitously found around the B1.5 I star Sher 25 in NGC 3603 (Figure 2, [20]). A search for circumstellar nebulae around  $>100$  B supergiants in the Galaxy and the Magellanic Clouds has yielded null results [21]. The similarity in spectral type between Sher 25 and Sk–69 202 and the similarity in the size and physical properties of their circumstellar rings suggest that Sher 25 is a Galactic twin of Sk–69 202 and may very well be on the verge of a SN explosion [22].

### *The Case of SNR 0540–69.3*

Next to SN 1987A, the second youngest SNR in the Large Magellanic Cloud (LMC) is SNR 0540–69.3 [23]. HST WFPC2 images of SNR 0540–69.3 in the  $H\alpha$  and [N II] lines show a [N II]-bright ring with a diameter of  $\sim 5''$ , or 1.25 pc (see Figure 3). Spectroscopic observations of the [N II] lines show narrow velocity profiles indicating an expansion velocity  $\leq 50 \text{ km s}^{-1}$  [23]. This [N II]-bright ring is apparently a circumstellar bubble of the SN progenitor. The size of this circumstellar nebula is comparable to those of LBV nebulae, but smaller than WR bubbles [14]. It is possible that the SN progenitor exploded during or shortly after an LBV phase. The elemental abundances of this circumstellar nebula need to be measured in order to confirm the LBV hypothesis.

**FIGURE 3.** **Left:** HST WFPC2 image of SNR 0540–69.3 in the  $[\text{N II}]\lambda 6583$  line. The circumstellar nebula is visible near the center of the PC field. **Right:** Chandra HRC X-ray image of SNR 0540–69.3. The X-ray emission peaks at the region of circumstellar nebula. These two images have the same image scales.

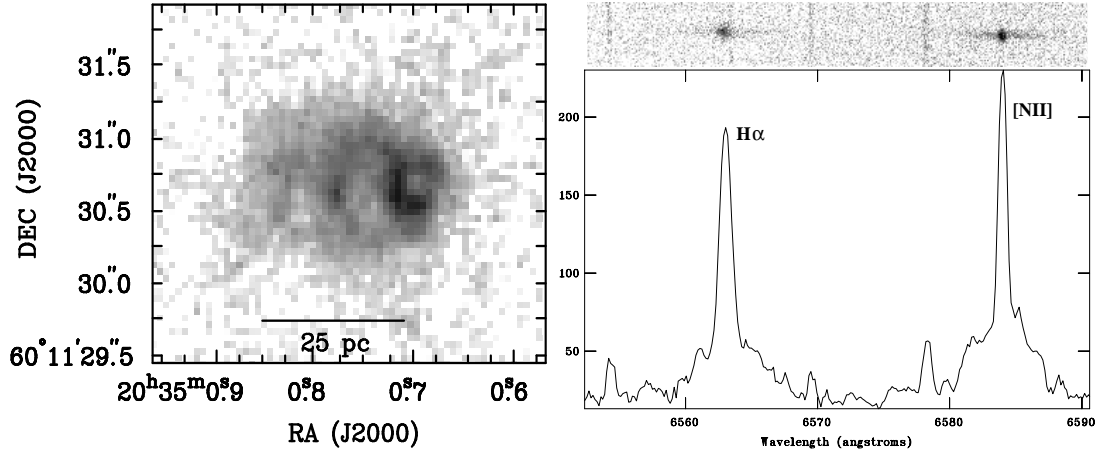


**FIGURE 4.** **Left:** HST WFPC2  $\text{H}\alpha$  image of MF 16 in NGC 6946. **Right:** Echellogram and profile plot of the  $\text{H}\alpha$ + $[\text{N II}]$  lines of MF 16 in NGC 6946. Both figures are taken from [28].

## *The Case of SNR MF16 in NGC 6946*

The SNR MF 16 in NGC 6946 [24] at a distance of  $\sim 5$  Mpc is known for its very high X-ray and optical luminosities, about 1,000 times as luminous as Cas A in X-rays [25,26]. HST WFPC2 images of MF 16 (Figure 4) show a multiple-loop morphology, which leads to the suggestion that the high luminosity of this remnant is caused by colliding SNRs. [27]. However, a different interpretation based on ground-based high-dispersion spectroscopic observations of MF 16 has been suggested [28]. The spectrum of MF 16 shows narrow  $H\alpha$  and  $[N\ II]$  lines superposed on the broad SNR components (Figure 4), and the  $[N\ II]/H\alpha$  ratio for the narrow component is high,  $\sim 1$ , indicating that the narrow components are emitted by N-enriched material. The expansion velocity implied by the velocity widths is  $< 15\text{ km s}^{-1}$ . It is thus possible that the narrow components originate in a circumstellar bubble and the collision between this circumstellar bubble and the SNR causes the high X-ray and optical luminosities. HST STIS long-slit observations of MF 16 are needed to examine the location of regions with high  $[N\ II]/H\alpha$  ratios in order to determine the boundary of the circumstellar bubble. Ground-based, kinematically-resolved spectrophotometric observations similar to those of NGC 6888 [29] are needed to determine the abundances of this circumstellar material.

### **3. Interstellar Bubbles**

Supernova ejecta in young SNRs, once having swept past the circumstellar material, can advance quickly to the inner walls of the interstellar bubble formed by the progenitor at the main sequence stage. The SNR N132D in the LMC is a good example [30]. The combination of high X-ray brightnesses and large linear sizes is usually indicative of such young SNRs. The detection/confirmation of an interstellar bubble is non-trivial, as illustrated in the example of N63A.

N63A is a SNR associated with the OB association LH83 in the LMC (Figure 5). Its optical image shows a three-lobed, clover-shaped nebulosity about  $20''$  ( $\sim 5$  pc) across. The two eastern lobes exhibit a high  $[S\ II]/H\alpha$  ratio, indicating a shock excitation, while the western lobe shows spectra characteristic of photoionization. The fact that N63A has such a high X-ray surface brightness and the fact that the optical size of the SNR N63A is much smaller than the extent of radio and X-ray emission ( $\sim 70''$ ) suggest that the SNR N63A is young and its SNR shock has just reached the inner walls of the progenitor's interstellar bubble.

HST WFPC2 images of N63A in  $H\alpha$  and  $[S\ II]$  resolved the filamentary structure in the two eastern lobes and diffuse emission in the western lobe, consistent with the excitation mechanisms diagnosed from their spectral properties [31]. Additionally, the WFPC2 images reveal a number of cloudlets as small as  $0.1$  pc across, within the X-ray-emitting regions of the SNR. The  $[S\ II]/H\alpha$  ratios and locations of these cloudlets suggest that these are shocked cloudlets lagging behind the shock front. These evaporating cloudlets are probably responsible for injecting mass into the

**FIGURE 5. Upper Left:**  $H\alpha$  image of N63, overlaid by X-ray contours extracted from a ROSAT HRI observation. This image shows that the SNR is associated with an OB association and embedded in an HII region. **Upper Right:** HST WFPC2 image of N63A in  $H\alpha$ . This image resolves not only the three bright lobes but also small cloudlets within the X-ray emission regions. **Lower Left:** Close-up of a small evaporating cloudlet. **Lower Right:** HST WFPC2 image of N63A in [O III]. The southern boundary of the SNR is delineated by a faint [O III] arc which is coincident with the X-ray boundary, suggesting that the [O III] arc marks the interstellar bubble blown by the supernova progenitor.

hot SNR interior to produce the high X-ray surface brightness. The  $H\alpha$  and [S II] images fail to show the location of the interstellar bubble.

A recent HST WFPC2 image of N63A in the [O III]  $\lambda 5007$  line finally shows a faint arc at the southern boundary of the SNR. The location of the arc coincides with the X-ray boundary. The long sought interstellar bubble of N63A is finally found.

## SUMMARY AND CONCLUSION

Young SNRs offer the best laboratories to study the archeological artifacts of massive supernova progenitors. It is possible to detect the very latest stellar ejecta (the deathbed ejecta), circumstellar nebulae ejected at late evolutionary stages, and interstellar bubbles blown by the progenitors at main sequence stage. Detailed spectroscopic observations of these nebulae are necessary to determine their abundances in order to assess the evolutionary stages of the progenitors right before the supernova explosion.

This research is partially supported the the HST grant STScIGO-08110.01-97A.

## REFERENCES

1. Walborn, N.R., Lasker, B.M., Laidler, V.G., & Chu, Y.-H., *ApJ* **321**, 41 (1987).
2. Podsiadlowski, P., *PASP* **679**, 717 (1992).
3. Chu, Y.-H. 1991, in IAU Symposium 143, Wolf-Rayet Stars and Interrelations with Other Massiv Stars in Galaxies, ed. K.A. van der Hucht and B. Hidayat (Dordrecht: Kluwer), p. 349
4. Chu, Y.-H. 1997, in CTIO/ESO/LCO Workshop "SN 1987A, Ten Years After," in press
5. Chu, Y.-H., Weis, K., & Garnett, D.R., *AJ* **117**, 1433 (1999).
6. Kirschner, R.P., & Chevalier, R.A., *ApJ* **218**, 142 (1977).
7. Langer, N., Hamann, W.-R., Lennon, M., Najarro, F., Pauldrach, A.W.A., Puls, J., *A&A* **290**, 819 (1994).



8. Humphreys, R.M., & Davidson, K., *ApJ* **232**, 409 (1979).
9. Weaver, R., McCray, R., Castor, J., Shapiro, P., & Moore, R., *ApJ* **218**, 377 (1977).
10. García-Segura, G., Mac Low, M.-M., & Langer, N., *A&A* **305**, 229 (1996).
11. García-Segura, G., Langer, N., & mac Low, M.-M., *A&A* **316**, 133 (1996).
12. Morse, J.A., Davidson, K., Bally, J., Ebbets, D., Balick, B., & Frank, A., *AJ* **116**, 2443 (1998).
13. Esteban, C., Vílchez, J.M., Smith, L.J., & Clegg, R.E.S., *A&A* **259**, 629 (1992).
14. Chu, Y.-H., Caulet, A., Montes, M.J., Panagia, N., Van Dyk, S.D., & Weiler, K.W., *ApJ* **512**, L51 (1999).
15. Salamanca, I., Cid-Fernandes, R., Tenorio-Tagle, G., Telles, E., Terlevich, R.J., & Munoz-Tunon, C., *MNRAS* **300**, L17 (1998).
16. Salamanca, I. 2000, in the 1999 May Symposium of the STScI, "The Greatest Explosions Since the Big Bang: Supernovae and Gamma-ray Bursts," eds. M. Livio, N. Panagia, K. Sahu, in press
17. Ryder, S., et al., *ApJ* **416**, 167 (1993).
18. Burrows, C.J., et al., *ApJ* **452**, 680 (1995).
19. Crotts, A.P.S., & Kunkel, W.E., *ApJ* **366**, L73 (1991).
20. Brandner, W., Grebel, E.K., Chu, Y.-H., & Weis, K., *ApJ* **475**, L45 (1997).
21. Chu, Y.-H., Brandner, W., & Grebel, E.K., presented in CTIO/ESO/LCO Workshop "SN 1987A, Ten Years After," in press (1997).
22. Brandner, W., Chu, Y.-H., Einsenhauer, F., Grebel, E.K., & Points, S.D., *ApJ* **489**, L153 (1997).
23. Caraveo, P.A., Mignani, R., & Bignami, G.F., *Mem. Soc. Astron. Italiana* **69**, 1061 (1998).
24. Matonick, D.M., & Fesen, R.A., *ApJS* **112**, 49 (1997).
25. Schlegel, E.M., *ApJ* **424**, L99 (1994).
26. Blair, W.P., & Fesen, R.A., *ApJ* **424**, L103 (1994).
27. Blair, W.P., Fesen, R.A., & Schlegel, E.M., *AJ*, submitted (2000).
28. Dunne, B.C., Gruendl, R.A., & Chu, Y.-H., *AJ* **119**, 1172 (2000).
29. Esteban, C., & Vílchez, J.M., *ApJ* **390**, 536 (1992).
30. Morse, J.A., et al., *AJ* **112**, 509 (1996).
31. Chu, Y.-H., et al., in IAU Symposium 190, "New Views of the Magellanic Clouds," p. 143 (1999).

This figure "fig3a.jpg" is available in "jpg" format from:

<http://arxiv.org/ps/astro-ph/0012520v1>

This figure "fig3b.jpg" is available in "jpg" format from:

<http://arxiv.org/ps/astro-ph/0012520v1>

This figure "fig5a.jpg" is available in "jpg" format from:

<http://arxiv.org/ps/astro-ph/0012520v1>

This figure "fig5b.jpg" is available in "jpg" format from:

<http://arxiv.org/ps/astro-ph/0012520v1>

This figure "fig5c.jpg" is available in "jpg" format from:

<http://arxiv.org/ps/astro-ph/0012520v1>

This figure "fig5d.jpg" is available in "jpg" format from:

<http://arxiv.org/ps/astro-ph/0012520v1>